Structural, Optical and Ultra-Violet Photodetection Properties of ZnO Nanorods with Various Aspect Ratios

Saeed Safa [1,*], Elham Hasani[2], Majid Zareh[2]
[1] *Young Researchers and Elite Club, South Tehran Branch, Islamic Azad University, Tehran, Iran*
[2] *Physics department, Karaj-branch, Islamic Azad University, Karaj, Iran*

ARTICLE INFO

Article history:

Received 7 July 2016
Accepted 5 September 2016
Available online 25 September 2016

Keywords:

ZnO nanorod
Optical characteristics
Ultra-violet photodetection

ABSTRACT

ZnO nanorods with various lengths were synthesized by a two-stage route (by changing the time of growth between 0-240 min) and were characterized using XRD, SEM, UV–Vis and PL techniques. The SEM and XRD results confirmed a fast growth of (0 0 2) plane in the preferential longitudinal orientation, in contrast to lateral growth and therefore, by increasing the time of hydrothermal growth, nanorods with higher aspect ratios are obtained. Naturally, by increasing the length of nanorods, not only the average transmittance in both near ultraviolet and visible ranges is decreased, but also the PL peaks are red-shifted and extinct. Finally, ultra-violet photodetection of the samples shows that higher active surface area (with respect to the time of growth) is appropriate for photo-induced interactions leading to higher UV-sensitivity.

1. Introduction

Among the various optoelectronic materials, zinc oxide has been tremendously studied due to its wide band-gap energy (~3.37 eV), large exciton binding energy (~60 meV), and facility of growing its nanostructures like nanorods (NRs) [1-4]. These outstanding intrinsic properties have made it the most promising material for a wide range of applications such as photonic crystals [1], transparent electrodes [2], ultraviolet (UV) light emitters [3], and photocatalyst materials [4]. In photo-assisted applications, ZnO acts as a sensitizer for light-induced interactions. For more explanation, the photo-assisted chain reaction involves (i) co-generation of electrons and holes (e/h) in conduction and valence bands by photo-excitation, (ii) transformation of photogenerated carriers in the circuit under the applied bias voltage (fast response mechanism), and (iii) the oxygen groups adsorption and desorption from the surface (slow response mechanism) [5]. Nevertheless, bulk ZnO suffers from its negligible photo-induced performance. Thus, some efforts have been made in order to regulate the photo-assisted properties of ZnO by changing its morphology [6] and doping by other additives [7]. Recently, Akhavan et al. [8] reported ZnO nanorods (NRs) as having the most favorable morphology for photocatalytic inactivation of E. Coli bacteria. Concerning the potential industrial applications of ZnO NRs as a famous UV detector, it is necessary to study the role of ZnO NR aspect ratio in its optical characteristics.

Accordingly, a number of studies have been published for controllable growth of ZnO NRs; i.e. vapor-phase transport [9, 10] pulsed laser deposition [11], chemical vapor deposition [12, 13], electrochemical deposition [14], hydrothermal growth of nanorods, and molecular beam epitaxy [15]. In this work, aqueous hydrothermal method was selected because of advantages like simplicity and low growth temperature, safety, cost-effectiveness, and especially controllability. ZnO NR arrays with various aspect ratios (by changing the growth time) were synthesized in a

* Corresponding author:
E-mail: sda.safa@gmail.com

hydrothermal bath and their optical and structural characteristics were analyzed and compared. Afterwards, the UV detecting performance of synthesized samples was evaluated by a purpose built apparatus.

2. Materials and methods

2.1. Preparation of ZnO NRs

At first, microscopic glass slides were cleaned by acetone, ethanol, and deionized water to remove contaminants. Afterward, ZnO thin film was spin-coated onto each clean glass substrate to prepare seed layer for NRs growth.

The spin-coating sol was prepared by a mixture of 0.05 M zinc acetate dihydrate and 0.06 M diethanolamine dissolved in ethanol. The solution was stirred at 60 °C for 20 min to become clear and homogeneous. Afterwards, the prepared sol was spin-coated onto the glass substrates at 3000 rpm for 30 sec. The coated films were dried at 180 °C for 10 min to evaporate the solvent and organic residuals. This procedure was repeated 5 times to produce a desired thickness of uniform ZnO film. Finally, the films were annealed at 500 °C for 1 h in air. Subsequently, after rinsing the ZnO seed layers by DI water, ZnO NRs were grown on seed layers by suspending them in a super-saturated aqueous solution of 0.001 M zinc nitrate and 0.1 M sodium hydroxide at 70 °C for 20, 40, 60, 120, and 240 minutes. Subsequently, the samples were cleaned by deionized water to remove the residual salts and annealed at 500 °C for 1 h.

2.2. Characterization

The surface morphology of the samples was depicted by scanning electron microscopy (SEM, VEGA, TESCAN). Also, due to the importance of seed layer topography and roughness for the growth of NRs, the seed-layer was studied by atomic force microscopy (AFM) using a Park Scientific model CP-Research (VEECO). The structural characterization of the samples was carried out via X-ray diffraction analysis (XRD) using an X'Pert PRO, Philips. The thickness of seed layer and NR thin films was evaluated by thickness profilemeter using a Stylus-Dektak. Room temperature photoluminescence spectra (PL) were taken on a PL-Perkin-Elmer LS55 equipped with a 450W Xe lamp as the excitation source.

2.3. UV-detecting study

UV photocurrent sensitivity of various samples was measured using a purpose-built dark box. The box has a vertically adjustable holder equipped with an 8 W Philips black-light UV-A lamp. The precise values of UV light as well as visible light intensities were measured by UV light meter Lutron 340A and visible light meter pro TES 1339R, respectively. To measure the conductivity and UV photoresponsivity, the comb-like gold terminals with a spacing of 1 mm were sputtered on each sample and copper wires were bonded to terminals by silver adhesive. The samples were connected to a known resistor in series and 2.0 V-DC was applied through the circuit. The DC voltage across the known resistor was read out using an A/D converter interfaced to computer for further processing. The purpose-built box was equipped with a shutter unit for ultrafast opening/closing of the light entrance aperture (Fig. 1).

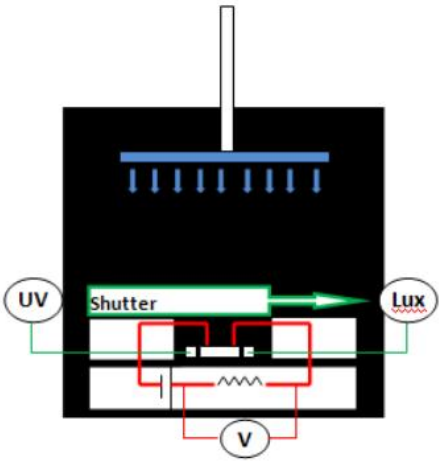

Fig.1. Schematic of the UV photocurrent sensitivity measuring box.

Fig. 2 shows the XRD patterns of the ZnO NR arrays grown in 20, 60 and 240 min. The X-ray diffraction peaks of ZnO NRs grown for 20 min are not clear and only very weak peaks are apparent. The lack of any preferential orientation for this sample revealed that NRs are still in the initial stage of growth [16]. Although the diffraction peaks of sample grown for 20 min are very weak, the 60 and 240 min grown samples show sharp peaks corresponding to (100), (002), (101), (102) planes, indicating that both of these samples are crystallized in a preferential texture of hexagonal wurtzite structure (JCPDS NO. 36-1451).

Quantitative information concerning the preferential crystal orientation can be obtained from the texture coefficient, TC, defined as equation (1) [18],

$$TC(hkl) = \frac{I(hkl)/I_0(hkl)}{(1/n)\sum_n I(hkl)/I_0(hkl)} \quad (1)$$

where I(hkl) is the observed intensity of the (hkl) plane, I0 (hkl) is the relative intensity of the corresponding plane given in the XRD reference (JCPDS 36-1451), and N is the total number of diffraction peaks.

With increasing the growth time, the above-mentioned ratio (TC) increased considerably and was estimated to be 0.14, 0.72 and 0.96 for NRs grown in 20, 60 and 240 min, respectively. Also, the mean crystallite sizes of the samples using the Scherrer equation were obtained ~19.01, 22.24, and 39.82 nm for the ZnO NRs grown in 20, 60, and 240 min, respectively. It can be observed that with increasing the time of equilibrium growth of NRs in the hydrothermal bath, both the length of NRs along the preferred orientation and the size of the crystallites increased. Moreover, as it was expected, the broad peak between 20°-35° originating from the amorphous glass substrate of samples gradually disappeared by thickening the ZnO NRs layer.

The surface morphology of the seed layer on glass substrate is shown by AFM micrograph in Fig. 3. The seed layer appears to be a dense film and almost without porosity with an average grain size ranging between 20 to 50 nm. The root mean square (RMS) surface roughness of the film was ~1.73 nm, indicating a nearly smooth and uniform layer for the growth of NRs.

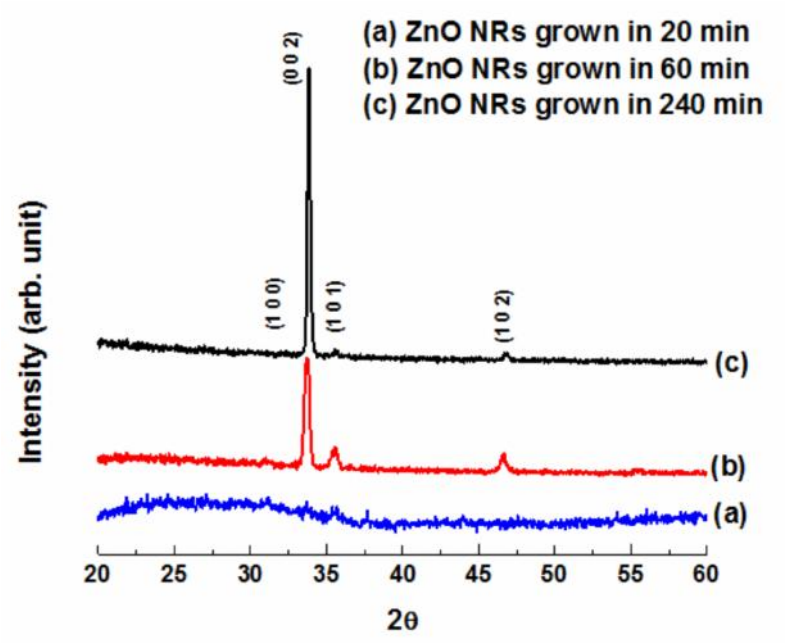

Fig. 2. The X-ray diffraction patterns of ZnO NRs grown in the hydrothermal bath for 20, 60, and 240min.

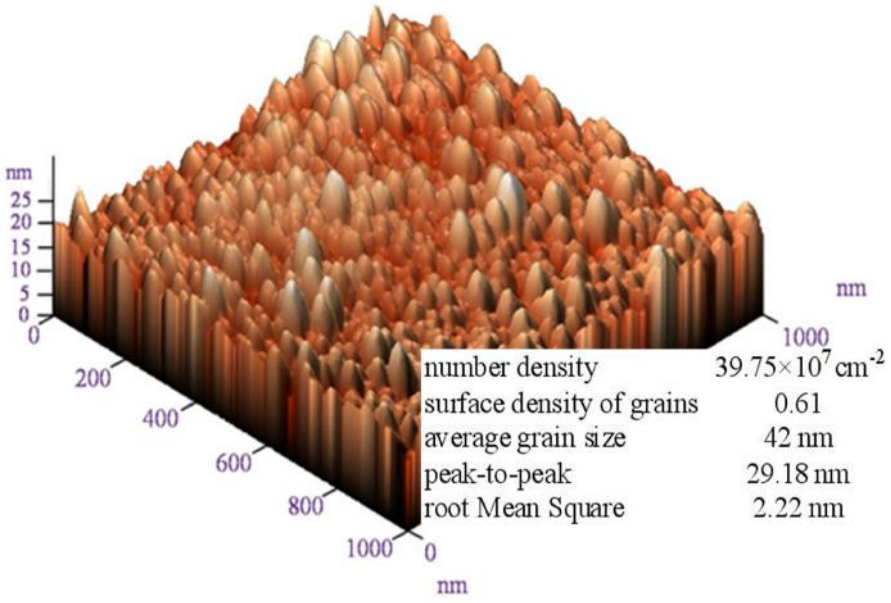

Fig. 3. AFM microghraph of ZnO seed layer.

Fig. 4 shows the SEM image of the NR arrays grown at various times. Obviously, for the sample grown for 20 min, it is hard to talk about the formation of ZnO nanorods. In fact, some occasional nano-features are seen in the image. It means that under the applied conditions for hydrothermal growth, the NRs are in the initial states for crystallization and growth (in good agreement with the XRD results).

With increasing the time of growth to 60 min, a close-packed array of NRs with an average diameter of ~ 80 nm is formed. Moreover, the SEM image of ZnO arrays shows that the growth direction of NRs is nearly toward the normal direction of the substrate. The growth mechanism of ZnO NRs in aqueous solution is based on heterogeneous nucleation and subsequent crystal growth on the seed layer. During the hydrothermal growth, an equilibrium point between the precipitation and etching reactions between supersaturated $Zn(NO_3)^{-2}$ and ZnO coated seed layer is established. In this state, $Zn(NO_3)_2$ hydrolyses in alkaline solution and forms the complexion $[Zn(OH)_n]^{2-n}$ (n = 2 or 4). Predominantly, the following reactions have been proposed for ZnO nanorods precipitation [8]:

$$2\left[Zn(OH)_n\right]^{2-n} \rightarrow \left[Zn_2O(OH)_{2n-2}\right]^{4-2n} + H_2O$$

With increasing the temperature up to 70 ^oC, the complexes dehydrate [V] on the surface of growing crystals which result in the heterogeneous growth at the interface between substrate and solution especially along with the most closely-pack direction [0001] with the lowest energy planes [17]. Accordingly, it could be seen that with increasing the growth time, the average NRs diameter obtained from SEM images is a little increased from ~ 80 nm to ~ 100 nm for NRs grown in 60 and 240 min, respectively, while the lengths of NRs obtained from Dektak were estimated ~ 85, 353, 895, 1250 and 1560 nm for 20, 40, 60, 120 and 240 min grown ZnO NR samples, respectively. Therefore, one can conclude that (002) plane is the preferential growth rather than any other planes. In this relation, Abbasi et al. [18] suggested that nitrate anions facilitate the preferential growth of high energy (002) plane

toward [0001] direction of ZnO unit cell in an alkaline growth solution.

Fig. 5 shows the room temperature photoluminescence (PL) spectra of ZnO NR films grown in 20, 60, and 240 min. To evaluate and compare the photoluminescence of each sample, the emission spectra were deconvoluted by Gaussian function to the four distinct peaks. The sharp peaks at ~402 nm are assigned to UV-emission due to the recombination of free excitons. The visible emissions at ~467 and 522 nm (blue and green emissions) mainly originate from the different defect states such as the existence of Zn-interstitials and O-vacancies in the lattice structure of ZnO. The broad emission band between 400-700 nm observed in all samples is assigned to the deep level emission band (DLE) [19]. It can be observed that the intensity of PL peaks decreased and UV-emission peak position is red-shifted from (λ = 397.5 nm, Intensity = 75.5 arb. u.) to (λ= 410.3 nm and Intensity = 8.66 arb. u.) with the increase of NR films thickness.

The UV-emisson red-shift could be explained by the regular multi-dispersity of incident light among the prolonged ZnO nanorods. Moreover, the increment of the defect induced peak to free exciton peak for NRs with higher aspect ratio (or length) could be due to an increased number of surface states occupied by lattice defects for longer NRs [19].

The transmittance and reflectance spectra of ZnO seed and NR films in the range of UV-Vis are shown in Fig. 5. The transmittance of the seed sample is about 90%, while it is decreased to about 60% for ZnO NR grown for 240 min. The decrement of optical transmittance is associated with light scattering and absorption by the surface of NRs [20-21].

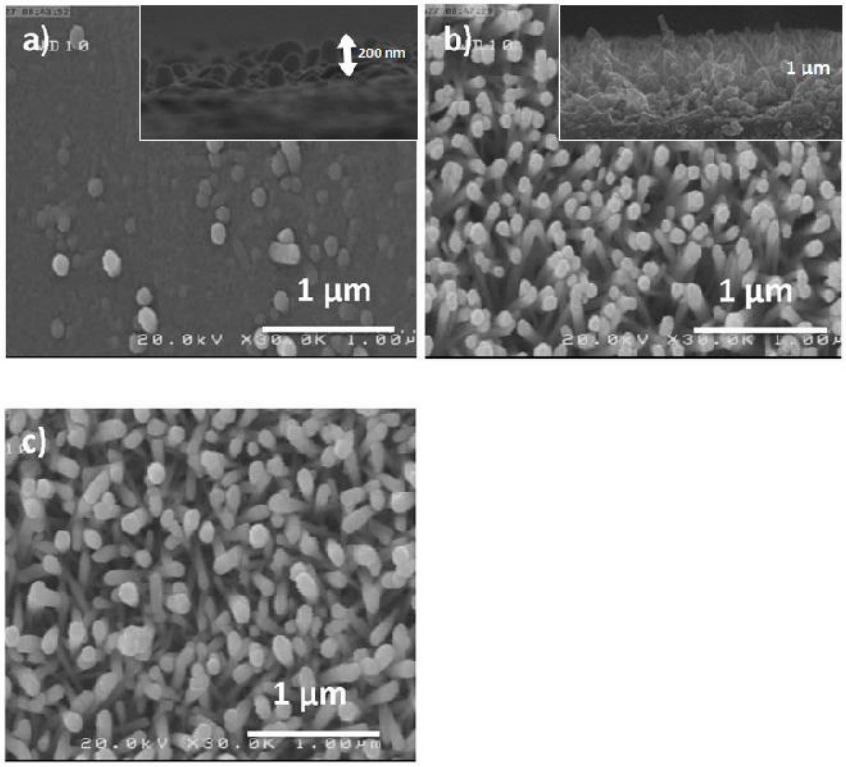

Fig.4. SEM images of NR films grown in the hydrothermal bath for a) 20, b) 60, and c) 240 min. The insets of (a) and (b) show the cross-sectional image of nanorods.

The band gap energy of the bare ZnO thin film was calculated from well-known tauc method [22] and it was found that by increasing the

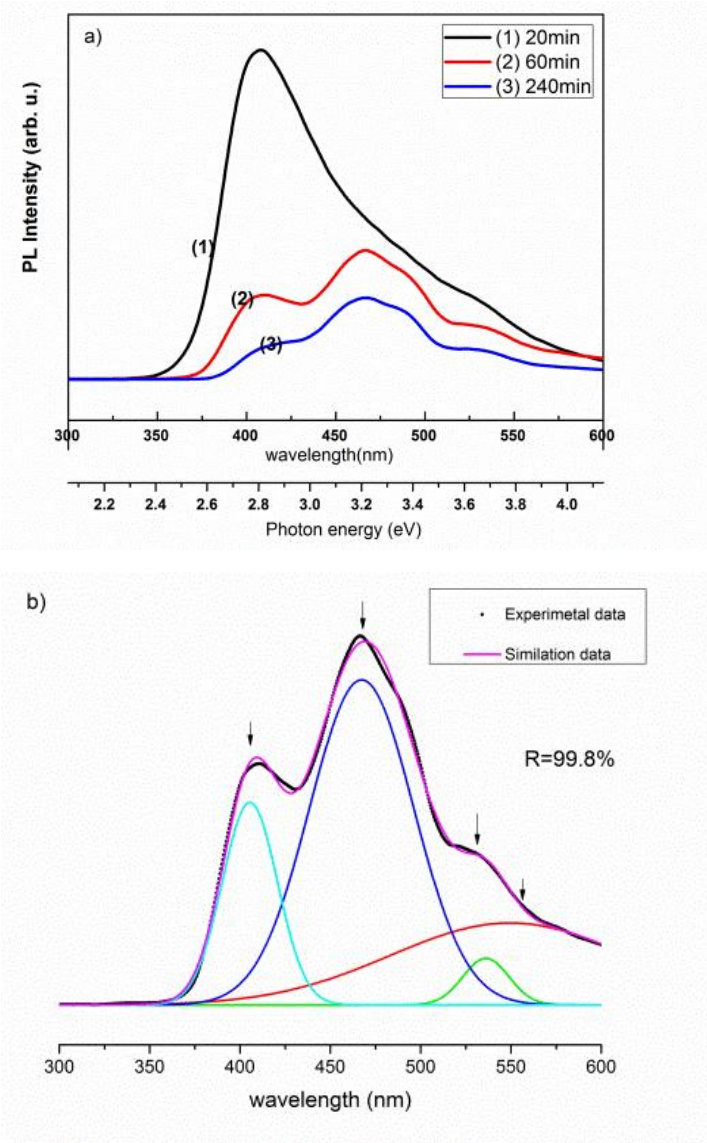

Fig.5. (a) Photoluminescence spectra of hydrothermally grown ZnO nanorods for various times of growth measured at room temperature and (b) deconvolution of the PL spectrum of ZnO nanorods grown for 60 min in the hydrothermal bath.

Fig. 7 presents the variation of photo-sensitivity of the samples under the same power of UV illumination. As can be seen, under the UV light, photocurrent increases rapidly to a certain value and then gradually becomes saturated. As the UV light is cut-off, the current tends to return to its initial state exponentially.

length of ZnO nanorods, the value of Eg decreases from ~3.3 to ~2.1 eV, which is obviously observable in optical transmittance spectra where the longer the length of nanorods, the higher the optical absorbance in both ultraviolet and visible range. As shown before [22], the decrease in the band gap can be

attributed to the multiple scattering and absorption of incident wavelength between lengthy nanorods.

time are increased with respect to the lengthening of ZnO nanorods. It is known that photo-sensitivity of ZnO is originated from two main reasons: i) photogenerated carriers

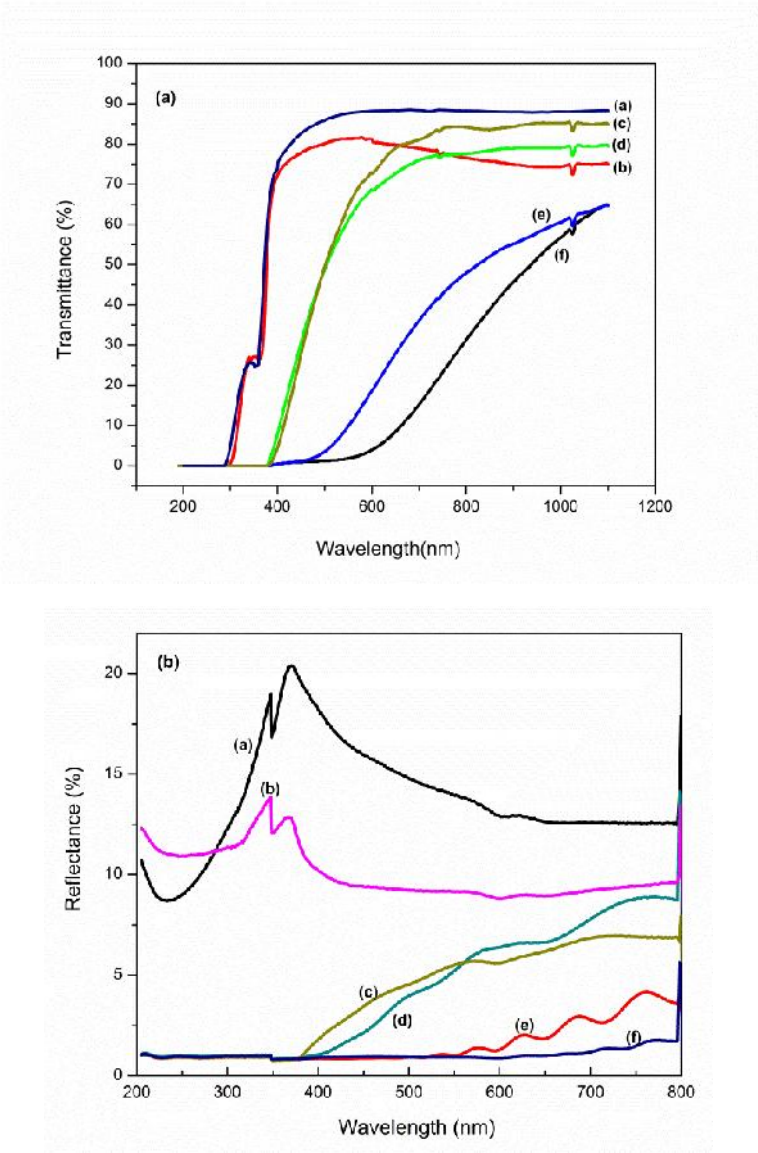

Fig. 6. Optical transmittance and reflectance spectra of ZnO a) seed layer, and hydrothermally synthesized NRs grown for b) 20, c) 40, d) 60, e) 120 and f) 240 min.

The sensitivity (Imax/Imin), t90-response (the time interval over which resistance attains the fixed 90% of the final value in plateau) and t90-recovery (the time interval over which resistance reduces to 10% of the saturated value) are shown in Fig. 7 and summarized in Table 1. As can be seen, both the photosensitivity and response

transformation in the circuit under the applied bias voltage (fast response mechanism), and (ii) the oxygen groups adsorption and desorption from the surface (slow mechanism). Moreover, it is known that photocurrent (Imax) is proportional to the number of photoexcited electron/hole pairs. Therefore, by increasing the

accessible surface of ZnO (lengthening the nanorods), higher photo-induced interactions (generation of electron/hole pairs and ads- and des-orption of oxygen groups) can be imagined on the surface of ZnO nanostructures. This result is in good agreement with transmittance and reflectance spectra of the samples, where the sample grown for 120 and 240 min showed the highest light absorbance through short wavelengths.

results showed that ultra-lengthened ZnO nanorods have higher optical absorbance.

On the other hand, obviously, higher density of photo-generated carriers need longer time to form (by UV illumination), transform through ZnO lattice structure and recombine (after light cut-off). The nearly similar results were reported by Ghosh et al. [40].

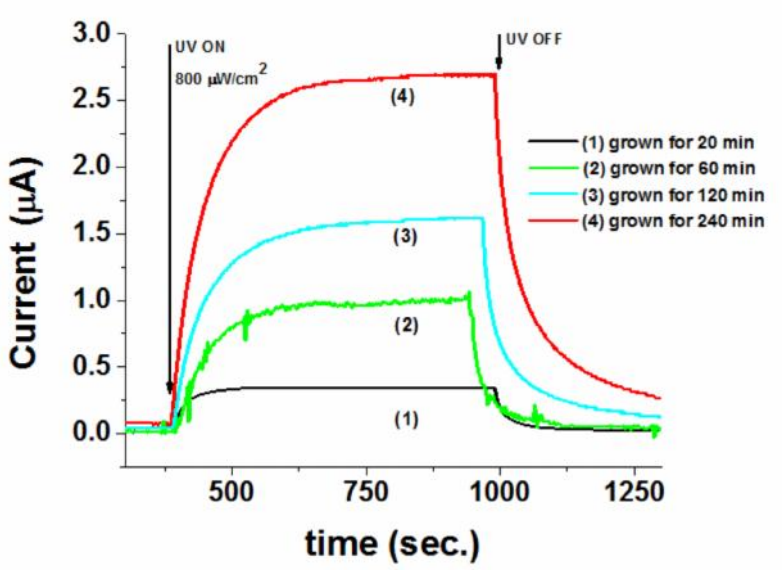

Fig.7. Ultra-violet detecting performance of ZnO nanorods grown at different times.

Table 1. Ultraviolet photo-sensitivity of the samples grown in various time.

Growth time	20	60	120	240
UV-sensitivity	17.5	33	40	45
Time of response (sec.)	74	170	177	184

4. Conclusions

This work provides a systematic study on the growth of ZnO nanorods arrays by hydrothermal method for various times. It was observed that nitrate anions cause the preferential growth of ZnO crystals toward [0001] direction in alkaline hydrothermal bath.

The crystallite size was found to be increased from ~19.01 to 39.82 nm with increase in the growth time from 20 to 240 min. The optical

The photodetecting analysis showed that by lengthening the NRs, photosensitivity and time of response are relatively increased. This could be attributed to the delayed surface photo-induced interactions which are directly coupled with the accessible surface.

References

[1] A. Janotti, C.G. Van de Walle, "Fundamentals of zinc oxide as a

semiconductor", Rep. Prog. Phys., Vol. 72, 2009, pp. 126501.

[2] V. Srikant, V. Sergo, D. R. Clarke, "Epitaxial Aluminum-Doped Zinc Oxide Thin Films on Sapphire: I, Effect of Substrate Orientation", J. Am. Ceram. Soc., Vol. 78, 1995, pp.1931-1934.

[3] Y. Ryu, T. S. Lee, J.A. Lubguban, H.W. White, B.J. Kim, Y.S. Park, C.J. Youn, "Next generation of oxide photonic devices: ZnO-based ultraviolet light emitting diodes", Appl. Phys. Lett., Vol. 88, 2006, pp. 241108-241108.

[4] H. Fu, T. Xu, S. Zhu, Y. Zhu, "Photocorrosion inhibition and enhancement of photocatalytic activity for ZnO via hybridization with C60", Environ. Sci. Technol., Vol. 21, 2008, pp. 8064.

[5] M. Mehrabian, R. Azimirad, K. Mirabbaszadeh, H. Afarideh, M. Davoudian, "UV detecting properties of hydrothermal synthesized ZnO nanorods." Physica E, Vol. 43, 2011, pp. 1141-1145

[6] Y. Liu, H. Lv, S. Li, X. Xing, G. Xi, "Preparation and photocatalytic property of hexagonal cylinder-like bipods ZnO microcrystal photocatalyst", Dyes Pigm., Vol. 95, 2012, pp. 443-449.

[7] J.H. Bang, S. Kenneth, "Applications of ultrasound to the synthesis of nanostructured materials", Adv. Mater., Vol. 22, 2010, pp.1039-1059.

[8] O. Akhavan, M. Mehrabian, K. Mirabbaszadeh, R. Azimirad, "Hydrothermal synthesis of ZnO nanorod arrays for photocatalytic inactivation of bacteria", J. Phys. D: Appl. Phys., Vol. 22, 2009, pp. 225-305.

[9] J. Zhang, Y. Su, H. Wei, J. Wang, C. Zhang, J. Zhao, Z. Yang, M. Xu, L. Zhang, Y. Zhang, "Double-nucleation hydrothermal growth of dense and large-scale ZnO nanorod arrays with high aspect ratio on zinc substrate for stable photocatalytic property", Mater. Lett., Vol. 107, 2013, pp. 251.

[10] W. Park, D. Hl Kim, S.W. Jung, G.C. Yi,"Metalorganic vapor-phase epitaxial growth of vertically well-aligned ZnO nanorods", Appl. Phys. Lett., Vol. 80, 2002, pp. 4232.

[11] Q. X. Zhao, P. Klason, M. Willander, "Growth of nanostructures by vapor liquid solid method", Appl. Phys. A, Vol. 88, 2007, pp. 27-30.

[12] M. H. Huang, Y. Wu, H. Feick, N. Tran, E. Weber, P. Yang, "Catalytic Growth of Zinc Oxide Nanowires by Vapor Transport", Adv. Mater., Vol. 13, 2001, pp. 113-116.

[13] Y. Sun, G. M. Fuge, M. N. R. Ashfold, "Growth of aligned ZnO nanorods arrays by catalysis-free pulsed laser deposition methods", Chem. Phys. Lett., Vol. 396, 2004, pp. 21-26.

[14] J. Wu, S.C. Liu, "Low-Temperature Growth of Well-Aligned ZnO Nanorods by Chemical Vapor Deposition", Adv .Mater., Vol. 14, 2002, pp.215-218.

[15] W.I. Park, D.H. Kim, S.W. Jung G.C. Yi, "Metalorganic vapor-phase epitaxial growth of vertically well aligned ZnO nanorods", Appl. Phys. Lett., Vol. 80, 2002, pp.4232-4234.

[16] H.D. Yu, Z.P. Zhang, M.Y. Han, X.T. Hao, F.R. Zhu, "A general low-temperature route for large-scale fabrication of highly oriented ZnO nanorod/nanotube arrays", J. Am. Chem. Soc., Vol. 127, 2005, pp. 2378-2379.

[17] J.X. Wang, X.W. Sun, Y. Yang, H. Huang, Y.C. Lee, O.K. Tan, L. Vayssieres, "Hydrothermally grown oriented ZnO nanorod arrays for gas sensing applications, Nanotechnol.", Vol. 19, 2006, pp. 4995.

[18] M.A. Abbasi, Y. Khan, S. Hussain, O. Nur, M. Willander, "Anions effect on the low temperature growth of ZnO nanostructures", J. Vac., Vol. 86, 2012, pp.1998-2001.

[19] B.J. Lawrie, R.F. Haglund, R. Mu, "Enhancement of ZnO photoluminescence by localized and propagating surface plasmons", Opt. Express, Vol. 17, 2009, pp. 2565-2572.

[20] A. Bakin, A. El-Shaer, A. Che Mofor, M. Kreye, A. Waag, F. Bertram, J. Christen, M. Heuken, J. Stoimenos, "MBE growth of ZnO layers on sapphire employing hydrogen peroxide as an oxidant", J. Cryst. Growth, Vol. 287, 2006, pp.7-11.

[21] O. Akhavan, R. Azimirad, S. Safa, M.M. Larijani, "Visible light photo-induced antibacterialactivity of CNT–doped TiO_2 thin films with various CNT contents", J. Mater. Chem., Vol. 20, 2010, pp. 7386.

[22] S. Safa, A. Khayatian, E. Rokhsat, M. Najafi, "Investigation of Structural, Optical,

and Photocatalytic Properties of Hydrothermally Synthesized ZnO Nanorod Arrays with Various Aspect Ratios", J. Adv. Mater. Proc., Vol. 20, 2016, pp. 51-64**.**